Optical properties of excitons in polar semiconductors: Energies, oscillator strengths, and phonon side bands

M. Matsuura* and H. Büttner†

Physikalisches Institut, Lehrstuhl für Theoretische Physik I, Universität Bayreuth, Postfach 3008, 8580 Bayreuth, West Germany

(Received 5 September 1979)

The optical properties of Wannier excitons interacting with LO phonons are discussed in terms of the oscillator strengths and optical-absorption coefficients. The quantities were calculated for the zero-phonon line and their phonon side bands in single-photon absorption as well as two-photon absorption. General properties of the optical spectra are described for the ground state and the first excited states. Numerical results for the cuprous halides and cuprous oxide compare satisfactorily with experimental data.

I. INTRODUCTION

The optical spectra of polar semiconductors provide a rich variety of information about the electronic states of the materials and their interaction with phonons. Besides the energies of the excitonic system one can determine the oscillator strength of the various transitions and their phonon side bands. The theoretical investigations started with the work of Haken[1] who gave a nice qualitative explanation for the effective interaction between an electron and a hole in a polar material. More recently a thorough quantitative discussion of the problem has been given in Refs. 2–4. The results for the ground-state energy of the relatively simple variational approach are in good agreement with other more involved methods and with experimental data.[3,5,6] To our knowledge there exists no comparable quantitative work for the other properties, like oscillator strengths[7,8] and phonon side bands.[9–12] The calculation of these quantities should give a much more stringent test to the excitonic wave function than it is possible with the determination of energies. In a recent communication[13] the method of Pollmann and one of the authors[2] (referred to PB hereafter) has therefore been extended to a study of these quantities in allowed transitions in single photon absorption (SPA) measurements and the agreement with experiments on CuCl and CuBr was satisfactory. In the present work we will extend these calculations to forbidden single photon absorption and allowed two photon absorption (TPA). In Sec. II energies and wave functions for the exciton-phonon system are obtained for any internal state of an exciton. From these oscillator strengths and optical absorption coefficients of zero phonon lines and their phonon side bands were calculated in Sec. III. In Sec. IV general properties of the results of Secs. II and III are discussed as functions of the various physical parameters. In Sec. V results are applied to cuprous halides (CuCl, CuBr, and CuI) and cuprous oxide. The final summary is given in Sec. VI.

II. ENERGY AND WAVE FUNCTION OF THE EXCITON-PHONON SYSTEM

We consider a nondegenerate isotropic two-band model for a Wannier exciton interacting with the LO phonon. The Hamiltonian for the system is written as

$$\tilde{H} = \frac{P^2}{2M} + \frac{p^2}{2\mu} + V(\vec{r}) + \sum_{\vec{k}} \hbar\omega a_{\vec{k}}^{\dagger} a_{\vec{k}} + \sum_{\vec{k}} \hbar\omega [v_{\vec{k}} \rho_{\vec{k}}(\vec{r}) e^{i\vec{k}\cdot\vec{R}} a_{\vec{k}} + \text{H.c.}] \tag{2.1}$$

$$\rho_{\vec{k}}(\vec{r}) = \exp(i s_2 \vec{k}\cdot\vec{r}) - \exp(-i s_1, \vec{k}\cdot\vec{r}),$$

$$s_i = m_i/M \quad (i = 1, 2) \tag{2.2}$$

and the interaction

$$\hbar\omega v_{\vec{k}} = -i(2\pi e^2 \hbar\omega / V\epsilon^* k^2)^{1/2}, \quad (\epsilon^*)^{-1} = \epsilon_\infty^{-1} - \epsilon_0^{-1}. \tag{2.3}$$

Here the center-of-mass (c.m.) motion and the relative motion of the exciton are described by the first three terms, where $M = m_1 + m_2$, $\mu = m_1 \cdot m_2/M$ with the electron mass m_1 and the hole mass m_2, and $\vec{P}$, $\vec{p}$, and $\vec{R}$, $\vec{r}$ are c.m. and relative momenta and coordinates, respectively. The potential $V(\vec{r}) = -e^2/\epsilon_\infty r + J\delta(\vec{r})$ represents the Coulomb plus exchange interaction (with the constant parameter J). The $a_{\vec{k}}^{\dagger}(a_{\vec{k}})$ is the creation (annihilation) operator of the LO phonon with the wave vector $\vec{k}$ and $\hbar\omega$ is the LO phonon energy.

Following PB, the following two unitary transformations were performed:

$$U_1 = \exp\left[i\left(\vec{Q} - \sum_{\vec{k}} \vec{k} a_{\vec{k}}^{\dagger} a_{\vec{k}}\right)\cdot\vec{R}\right] \tag{2.4}$$

and

$$U_2 = \exp\left(\sum_{\vec{k}} [F^*_{\vec{k}}(\vec{r}) a_{\vec{k}} - F_{\vec{k}}(\vec{r}) a^\dagger_{\vec{k}}]\right) \tag{2.5}$$

with the choice of

$$F_{\vec{k}}(\vec{r}) = v^*_{\vec{k}} [f^1_{\vec{k}} \exp(-is_2 \vec{k}\cdot\vec{r}) - f^2_{\vec{k}} \exp(is_1 \vec{k}\cdot\vec{r})]. \tag{2.6}$$

The total momentum of the exciton-phonon system $\vec{Q} = \vec{P} + \sum_{\vec{k}} \vec{k} a^\dagger_{\vec{k}} a_{\vec{k}}$ is a constant of motion. The first transformation U_1 eliminates the c.m. coordinate $\vec{R}$. The second transformation shifts the phonon coordinate as seen from $U_2^{-1} a^\dagger_{\vec{k}} U_2 = a^\dagger_{\vec{k}} - F^*_{\vec{k}}(\vec{r})$ and the amount of the displacement will be determined later. The transformed Hamiltonian H and the wave function $|\Phi\rangle$ are given by

$$H = U_2^{-1} U_1^{-1} \tilde{H} U_1 U_2 \tag{2.7}$$

and

$$|\Phi\rangle = U_2^{-1} U_1^{-1} |\Psi\rangle. \tag{2.8}$$

Here $|\Psi\rangle$ is the original wave function corresponding to $\tilde{H}$. For the discussion of optical absorption, one may set $\vec{Q} = 0$. Using the product ansatz $|\Phi\rangle = \psi_n(\vec{r})|0\rangle$, where $\psi_n(\vec{r})$ is the wave function of the relative motion specified by n, and $|0\rangle$ is the phonon vacuum state, the state-dependent variational parameters $f^i_{\vec{k}}$ have been determined in PB by minimizing the expectation value of H. Under the reasonable assumption of a symmetric charge distribution $|\psi_n(\vec{r})|^2 = |\psi_n(-\vec{r})|^2$, we may easily keep the state dependency of $f^i_{\vec{k}}$ for any internal state n and obtain

$$f^{i,n}_{\vec{k}} = \frac{[1 - G^n(\vec{k})][1 + R_j^2 k^2 + G^n(\vec{k})]}{(1 + R_i^2 k^2)(1 + R_j^2 k^2) - [G^n(\vec{k})]^2}$$

$$i \neq j = 1, 2, \tag{2.9}$$

where the polaron radius $R_j = (\hbar/2\omega m_j)^{1/2}$ and $G^n(\vec{k}) = \int d^3r |\psi_n(\vec{r})|^2 \exp(i\vec{k}\cdot\vec{r})$. In the following we will suppress one of the upper indices of $f^{i,n}_{\vec{k}}$, n, for brevity.

For the $f^i_{\vec{k}}$ in (2.9) the Hamiltonian H is given by

$$H = H_{ex} + H_{ph} + H', \tag{2.10}$$

$$H_{ex} = \frac{p^2}{2\mu} + V(r) - 2\hbar\omega \sum_{i,\vec{k}} |v_{\vec{k}}|^2 [f^i_{\vec{k}} - (f^i_{\vec{k}})^2 (1 + R_i^2 k^2)/2]$$

$$+ 2\hbar\omega \sum_{\vec{k}} |v_{\vec{k}}|^2 (f^1_{\vec{k}} + f^2_{\vec{k}} - f^1_{\vec{k}} f^2_{\vec{k}}) \cos(\vec{k}\cdot\vec{r}) \tag{2.11}$$

and

$$H_{ph} = \sum_{\vec{k}} (\hbar\omega + \hbar^2 k^2/2M) a^\dagger_{\vec{k}} a_{\vec{k}}, \tag{2.12}$$

$$H' = \sum_{\vec{k}} [H_1(\vec{k}) a^\dagger_{\vec{k}} + \text{H.c.}]$$

$$+ \sum_{\vec{k},\vec{q}} [H_2(\vec{k},\vec{q}) a^\dagger_{\vec{k}} a_{\vec{q}} + H_2'(\vec{k},\vec{q}) a^\dagger_{\vec{k}} a^\dagger_{\vec{q}} + \text{H.c.}]$$

$$+ H_3 + H_4, \tag{2.13}$$

where the various coefficients are defined as follows:

$$H_1(\vec{k}) = \hbar\omega v^*_{\vec{k}} \{[1 - (1 + R_1^2 k^2) f^1_{\vec{k}}] \exp(-is_2 \vec{k}\cdot\vec{r})$$
$$- [1 - f^2_{\vec{k}} (1 + R_2^2 k^2)] \exp(is_1 \vec{k}\cdot\vec{r})$$
$$+ [f^1_{\vec{k}} \exp(-is_2 \vec{k}\cdot\vec{r})/m_1$$
$$+ f^2_{\vec{k}} \exp(is_1 \vec{k}\cdot\vec{r})/m_2] \vec{k}\cdot\vec{p}/\omega\}, \tag{2.14}$$

$$H_2(\vec{k},\vec{q}) = v^*_{\vec{k}} v_{\vec{q}} \hbar^2 \vec{k}\cdot\vec{q} \{f^1_{\vec{k}} f^{1*}_{\vec{q}} \exp[-is_2(\vec{k} - \vec{q})\cdot\vec{r}/m_1$$
$$+ f^2_{\vec{k}} f^{2*}_{\vec{q}} \exp[is_1(\vec{k} - \vec{q})\cdot r]/m_2\}, \tag{2.15}$$

$$H_2'(\vec{k},\vec{q}) = v^*_{\vec{k}} v^*_{\vec{q}} k^2 \vec{k}\cdot\vec{q}\, \tfrac{1}{2} \{f^1_{\vec{k}} f^1_{\vec{q}} \exp[-is_2(\vec{k} + \vec{q})\cdot\vec{r}]/m_1$$
$$+ f^2_{\vec{k}} f^2_{\vec{q}} \exp[is_1(\vec{k} + \vec{q})\cdot\vec{r}]/m_2\}, \tag{2.16}$$

$$H_3 = -\sum_{\vec{k},\vec{q}} \{v^*_{\vec{q}} \hbar^2 \vec{k}\cdot\vec{q} [f^1_{\vec{q}} \exp(-is_2 \vec{q}\cdot\vec{r})$$
$$- f^2_{\vec{q}} \exp(is_1 \vec{q}\cdot\vec{r})]/M\} a^\dagger_{\vec{q}} a^\dagger_{\vec{k}} a_{\vec{k}} + \text{H.c.}, \tag{2.17}$$

$$H_4 = \sum_{\vec{k},\vec{q}} (\hbar^2 \vec{k}\cdot\vec{q}/2M) a^\dagger_{\vec{k}} a^\dagger_{\vec{q}} a_{\vec{k}} a_{\vec{q}}. \tag{2.18}$$

The first two terms of H, H_{ex}, and H_{ph} are diagonal with respect to the exciton relative motion and the phonon state. In the present work we will consider only these diagonal terms. The off-diagonal term H' may be quite important for interference effects of two exciton-phonon states. In some cases exciton-phonon bound states[14] may be expected. These problems are neglected for the moment and will be discussed in a forthcoming paper.

For H_{ex} the eigenfunction $\psi_n(\vec{r})$ with energy E_n is calculated variationally from $E_n = \langle \psi_n | H_{ex} | \psi_n \rangle$. For H_{ph} the wave function $|m\rangle$ and the corresponding energy E_m are given by

$$|m\rangle = \prod_{\vec{k}} \frac{(a^\dagger_{\vec{k}})^{n_{\vec{k}}}}{(n_{\vec{k}}!)^{1/2}} |0\rangle,$$
$$E_m = \sum_{\vec{k}} \left(\hbar\omega + \frac{h^2 k^2}{2M}\right) n_{\vec{k}} \tag{2.19}$$

under the condition $\sum_{\vec{k}} n_{\vec{k}} = m$, where $n_{\vec{k}}$ is the occupation number of the LO phonon with the wave vector $\vec{k}$. It should be noted that the phonon state

is specified by the distribution of the $n_{\vec{k}}$. The corresponding total wave functions and energies are

$$\Psi_{n,m} = U_1 U_2 \psi_n(\vec{r}) |m\rangle , \quad E_{n,m} = E_n + E_m . \tag{2.20}$$

III. OSCILLATOR STRENGTH AND OPTICAL ABSORPTION COEFFICIENT

Characteristic quantities for the optical absorption are the oscillator strength f and the optical absorption coefficient α of the various transitions. In this chapter we will calculate these quantities, using the energy and the wave function obtained in the previous section. At first we consider a single photon absorption (SPA). For a transition from the ground state E_0 to the excited state $E_{n,m}$, one obtains (cf. Refs. 14 and 15)

$$f = c_f \sum_{n,m} |P^{(1)}_{n,m}|^2 \tag{3.1}$$

and

$$h\nu\alpha(h\nu) = c_\alpha \sum_{n,m} |P^{(1)}_{n,m}|^2 \delta(E_{n,m} - E_0 - h\nu) , \tag{3.2}$$

where c_f and c_α are constants and $h\nu$ is the energy of the photon. The optical transition matrix element $P^{(1)}_{n,m}$ is given by

$$P^{(1)}_{n,m} = \sum_{\vec{q}} \vec{\epsilon} \cdot \vec{M}^*_{cv}(\vec{q}) \langle 0 | A_{n,m}(\vec{q}, -\vec{q}) | 0 \rangle , \tag{3.3}$$

where $\vec{\epsilon}$ is the polarization vector of the photon and $\vec{M}_{cv}(\vec{q})$ is the optical transition matrix element between the conduction and valence electrons. The amplitude $A_{n,m}(\vec{k}, \vec{q})$ is given by the Fourier transformation of the total wave function $\Psi_{n,m}$:

$$\Psi_{n,m} = \sum_{\vec{k},\vec{q}} \exp[i(\vec{k}+\vec{q})\cdot\vec{R}] \exp[i(\vec{k}s_2 - \vec{q}s_1)\cdot\vec{r}] \times A_{n,m}(\vec{k}, \vec{q}) |0\rangle . \tag{3.4}$$

According to the nonzero value of $\vec{M}_{cv}(q=0)$ the nature of the optical transition is different. The case $\vec{M}_{cv} \equiv \vec{M}_{cv}(q=0) \neq 0$ is called the allowed transition, while the case $\vec{M}_{cv} = 0$ and $(\partial \vec{M}_{cv}/\partial \vec{q})_{\vec{q}=0} \neq 0$ is called the forbidden transition.[15]

For both cases the oscillator strength and the optical absorption coefficient may be calculated from (3.3). For convenience these quantities may be rewritten as a sum of the individual contribution from the excited state n, m. The oscillator strength and the absorption coefficient may be written as

$$f = \sum_n f_n = \sum_n \sum_{i=0}^{\infty} f_n^{(i)} , \tag{3.5}$$

and

$$\alpha(h\nu) = \sum_n \alpha_n(h\nu) = \sum_n \sum_{i=0}^{\infty} \alpha_n^{(i)}(h\nu) . \tag{3.6}$$

Here $f_n^{(0)}$ and $\alpha_n^{(0)}(h\nu)$ are due to the zero phonon line of the exciton state $\Psi_n(\vec{r})$, while $f_n^{(m)}$ and $\alpha_n{}^m(h\nu)$ for $m \geq 1$ are due to its m-phonon side band. It has been assumed that the sum over all possible configurations involving m phonons has been performed in each m-phonon side band.

In the case of allowed transition we may obtain

$$P^{(1)}_{n,m} = \vec{\epsilon} \cdot \vec{M}^*_{c,v} \exp(-g_n/2) \left\langle 0 \left| \exp\left[\sum_{\vec{k}} F^*_{\vec{k}}(0) a_{\vec{k}}\right] \right| m \right\rangle \times \psi_n(0) , \tag{3.7}$$

where g_n is given by

$$g_n = \sum_{\vec{k}} |F_{\vec{k}}(0)|^2 = \sum_{\vec{k}} |v_{\vec{k}}|^2 (f^1_{\vec{k}} - f^2_{\vec{k}})^2 . \tag{3.8}$$

Note that g_n is a state-dependent quantity since $f^i_{\vec{k}}$ is state dependent. After averaging over the different polarizations of the photon, we obtain the following results for $f_n^{(i)}$ and $\alpha_n^{(i)}(h\nu)$ $(i = 0, 1, 2)$[13]:

$$f_n^{(0)} = A |\psi_n(0)|^2 \exp(-g_n); \quad f_n^{(1)} = f_n^{(0)} g_n; \quad f_n^{(2)} = f_n^{(0)} g_n^2/2 , \tag{3.9}$$

and

$$h\nu\alpha_n^{(0)}(h\nu) = B f_n^{(0)} \delta(E_g + E_n - h\nu) , \tag{3.10}$$

$$h\nu\alpha_n^{(1)}(h\nu) = B f_n^{(0)} \sum_{\vec{k}} |F_{\vec{k}}(0)|^2 \times \delta(E_g + E_n + \hbar\omega + \hbar^2 k^2/2M - h\nu), \tag{3.11}$$

$$h\nu\alpha_n^{(2)}(h\nu) = B f_n^{(0)} \sum_{\vec{k}\vec{q}} |F_{\vec{k}}(0) F_{\vec{q}}(0)|^2/2 \times \delta(E_g + E_n + 2\hbar\omega + \hbar^2(k^2+q^2)/2M - h\nu) . \tag{3.12}$$

The new constants A and B include the previous constants c_f, c_α, the dipole matrix element $\vec{M}_{cv}$, and the effect of the polarization. E_g is the band gap. The results of (3.9)–(3.12) indicate that in the allowed transition case only the s-exciton states and their phonon side bands are observed. The magnitude of the phonon side band depends on the value of g_n and thus is state dependent. Since g_n is zero for equal electron and hole masses, the phonon side bands are expected to be observed most easily in materials which have a small electron-to-hole mass ratio. While the zero-phonon state appears as a sharp line in the absorption spectra, phonon side bands have a broader structure whose shape depends on the exciton state n.

For the case of a forbidden transition the following $P^1_{n,m}$ are obtained from (2.20), (3.3), and (3.4):

$$P^{(1)}_{n,m}=\sum_l \vec{\epsilon}\cdot(\partial \vec{M}^{*}_{cv}/\partial q_l)_{\vec{q}=0}\{\partial[\langle 0|U_2|m\rangle\psi_n(\vec{r})]/\partial \vec{r}_l\}_{\vec{r}=0}\,, \tag{3.13}$$

where the sum of l is over x, y, and z. The oscillator strength $f^{(l)}_n$ and the absorption coefficient $\alpha^{(l)}_n(h\nu)$ have two different contributions

$$f^{(l)}_n=f^{(l)}_{n,p}+f^{(l)}_{n,s}\quad \alpha^{(l)}_n(h\nu)=\alpha^{(l)}_{n,p}+\alpha^{(l)}_{n,s}. \tag{3.14}$$

Here $f^{(l)}_{n,p}$ and $\alpha^{(l)}_{n,p}(h\nu)$ are unequal zero only for p states. After taking into account of possible three states for p states, these are given by

$$f^{(0)}_{n,p}=3A'|\partial\psi_n/\partial \vec{r}|^2_{\vec{r}=0}\exp(-g_n)\,,$$
$$f^{(1)}_{n,p}=f^{(0)}_{n,p}g_n,\quad f^{(2)}_{n,p}=f^{(0)}_{n,p}g_n^2/2\,, \tag{3.15}$$

and similar formulas as (3.10)–(3.12) with the replacement of $\alpha^{(l)}_{n,p}(h\nu)$, B', and $f^{(0)}_{n,p}$ instead of $\alpha_n{}^{l}(h\nu)$, B, and $f_n{}^{0}$, respectively. The constants A' and B' have absorbed the effect of polarization and the factor $\partial \vec{M}_{cv}/\partial \vec{q}_g$, being assumed to have the cubic symmetry. The other contributions in (3.14), $f^{(l)}_{n,s}$ and $\alpha^{(l)}_{n,s}(h\nu)$, are finite only for s-exciton states. Their first three terms are given by

$$f^{(0)}_{n,s}=0,\quad f^{1}_{n,s}=A'|\psi_n(0)|^2\exp(-g_n)g'_n,\quad f^{(2)}_{n,s}=f^{(1)}_{n,s}g_n \tag{3.16}$$

and

$$h\nu\alpha^{(0)}_{n,s}(h\nu)=0 \tag{3.17}$$

$$h\nu\alpha^{(1)}_{n,s}(h\nu)=B'|\psi_n(0)|^2\exp(-g_n)\sum_{\vec{k}}|\partial F_{\vec{k}}(\vec{r})/\partial \vec{r}|^2_{\vec{r}=0}\,\delta(E_g+E_n+\hbar\omega+\hbar^2k^2/2M-h\nu)\,, \tag{3.18}$$

$$h\nu\alpha^{(2)}_{n,s}(h\nu)=B'|\psi_n(0)|^2\exp(-g_n)\sum_{\vec{k},\vec{q}}|\partial F_{\vec{k}}(\vec{r})F_q(\vec{r})/\partial \vec{r}|^2_{\vec{r}=0}/2\,\delta(E_g+E_n+2\hbar\omega+\hbar^2(k^2+g^2)/2M-h\nu). \tag{3.19}$$

The new factor for phonon side bands g'_n is written as

$$g'_n=\sum_{\vec{k}}|\partial F_{\vec{k}}(\vec{r})/\partial \vec{r}|^2_{\vec{r}=0}=\sum_{\vec{k}}|v_{\vec{k}}|^2k^2(s_2f^1_{\vec{k}}+s_1f^2_{\vec{k}})^2. \tag{3.20}$$

The expressions for $f^{(l)}_{n,p}$ and $\alpha^{(l)}_{n,p}$ are similar to those in the allowed case except the factor $|\partial\psi_n(\vec{r})/\partial \vec{r}|^2_{\vec{r}=0}$ instead of $|\psi_n(0)|^2$. The contributions arising from $f^{(l)}_{n,s}$, $\alpha^{(l)}_{n,s}$ are quite different in nature. They include a derivative of $\langle 0|U_2|m\rangle$ with respect to $\vec{r}$ in (3.13) and represent the indirect process to the phonon side band of the s exciton. The zero-phonon line is missing and only the phonon side bands are possible. Their magnitude depends on the quantity g_n and g'_n. It may be noticed that g'_n is finite for any mass ratio unlike g_n. Thus the phonon side bands of the s exciton in a forbidden transition may be quite different from those in a direct transition.

In a final step we will consider briefly the optical absorption coefficient $\alpha(h\nu_1, h\nu_2)$, due to the TPA in the case of allowed transitions, using two band models.[16] Suppose that there are two different photon beams: a laser with the fixed energy $h\nu_1$ and the polarization vector ϵ_1, and a weak and continuous lamp, whose energy and polarization vector are denoted by $h\nu_2$ and ϵ_2. The absorption coefficient $\alpha(h\nu_1, h\nu_2)$ is written as[16-18]

$$\alpha(h\nu_1,h\nu_2)=c'_\alpha/\nu_1^2\nu_2\sum_{n,m}|P^{(2)}_{n,m}|^2\delta(E_{n,m}-E_0-h\nu_1 h\nu_2)\,. \tag{3.21}$$

with the transition matrix element $P^{(2)}_{n,m}$ which describes the transition from the ground state E_0 to the excited state $E_{n,m}$ through intermediate states.

In the calculation of the transition matrix element $P^{(2)}_{n,m}$, the sum over the intermediate states is rather difficult. In the case of a pure Wannier exciton model having a hydrogenic series of energies, the sum can be performed exactly with the use of the Coulomb-Green function.[16,18] However, under the influence of the LO phonon the energies and the wave functions of the exciton state change considerably and the exact summation seems not to be feasible. In the present work a simple approximation is used. The energy denominator $E_{n,m}-E_0$ is replaced by some average value ΔE, which is independent of the intermediate state n', m'.[1,16] Using the completeness of the intermediate state, $P^{(2)}_{n,m}$ reduces to

$$P^{(2)}_{n,m}=\vec{\epsilon}_1\cdot\vec{M}_{cv}\vec{\epsilon}_2\cdot[\partial\langle 0|U_2|m\rangle\psi_n(\vec{r})/\partial \vec{r}]_{\vec{r}=0}\times\frac{m\hbar}{\mu}\frac{1}{\Delta E-h\nu_1}+(1\rightleftharpoons 2) \tag{3.22}$$

in the allowed transition case. If the polarizations are parallel, we obtain

$$\alpha(h\nu_1,h\nu_2)=c''_\alpha/\nu_1^2\nu_2\sum_{n,m}[\partial\langle 0|U_2|m\rangle\psi_n(\vec{r})/\partial \vec{r}]_{\vec{r}=0}\times\delta(E_{n,m}-E_0-h\nu_1-h\nu_2)\,, \tag{3.23}$$

where the new constant c''_α has absorbed the previous constant c'_α, the effect of the polarization, and the factor $[(\Delta E - h\nu_1)^{-1} + (\Delta E - h\nu_2)^{-1}]^2$. Therefore, within our approximation the two-photon absorption spectra for the allowed transition is similar to the one-photon absorption spectra in the forbidden case. Defining the oscillator strength of the TPA being proportional to the right-hand side of (3.23) without $\nu_1^2\nu_2$ and the delta function, we may use the same formulas for the oscillator strength and the absorption coefficient as in the forbidden transition of SPA in the discussion of properties of TPA.

In the hydrogenic Wannier exciton case, the present type average energy denominator approximation has been shown to be reasonably good when

$$E_B/(E_g - h\nu_\alpha) = k_\alpha^2, \quad \alpha = 1,2 \tag{3.24}$$

is much smaller than one ($k_\alpha \lesssim 0.5$), where E_B is the binding energy of the exciton.[16] This criterion may be also used in the present case as a rough guidance for the validity of the approximation.

IV. GENERAL PROPERTIES OF AN EXCITON POLARON

In the present section general properties of an exciton under the influence of the LO phonon are discussed. If the exchange potential is neglected for the moment, our system is characterized by the following four physical parameters: The reduced mass in units of the free electron mass (m) μ/m, the electron-hole mass ratio $\sigma = m_1/m_2$, the strength of the Coulomb binding in units of the phonon energy $\mathcal{R}_\infty/\hbar\omega = \mu e^4/2\hbar^3\epsilon_\infty^2\omega$, and the Fröhlich electron-phonon coupling constant $\alpha = e^2(m/2\hbar^3\omega)^{1/2}/\epsilon^*$. These parameters are given in Table I for various semiconductors. Actually these four parameters are not completely independent. Defining the static Rydberg energy $\mathcal{R}_0 = \mu e^4/2\hbar^2\epsilon_0^2$, the following relation is valid: $(\mathcal{R}_0/\hbar\omega)^{1/2} = (\mathcal{R}_\infty/\hbar\omega)^{1/2} - \alpha(\mu/m)^{1/2}$. Since both sides should be positive, this restricts the range of the parameter values.

For a given set of parameters the eigenfunction $\psi_n(\vec{r})$ and the eigenenergy E_n are calculated variationally. The following ansatz for the wave functions is used in our calculation for $1s$, $2s$, $3s$, $2p$, and $3p$ states:

$$\begin{aligned}
\psi_{1s}(\vec{r}) &= N_{1s}\exp(-\alpha_s r),\\
\psi_{2s}(\vec{r}) &= N_{2s}(1 - A_2 r)\exp(-\beta_s r),\\
\psi_{3s}(\vec{r}) &= N_{3s}(1 - A_3 r + B_3 r^2)\exp(-\gamma_s r),\\
\psi_{2p}(\vec{r}) &= N_{2p} r\cos\Theta\exp(-\beta_p r),\\
\psi_{3p}(\vec{r}) &= N_{3p}(r - C_3 r^2)\cos\Theta\exp(-\gamma_p r).
\end{aligned} \tag{4.1}$$

TABLE I. Values of physical parameters used in the present work for several polar semiconductors; the reduced bare mass μ/m, the electron-phonon coupling constant α, the strength of the Coulomb binding $\mathcal{R}_\infty/\hbar\omega = \mu e^4/2\hbar^3\epsilon_\infty^2\omega$, the electron-hole mass ratio σ, the electron polaron radius R_1, the hole polaron radius R_2, and $1s$ exciton radius $r_{1s} = 1.5(m\hbar\omega/\mu\mathcal{R}_\infty)^{1/2}$. All lengths are in units of $R_{\text{free}}[= (\hbar/2m\omega)^{1/2}] = 1$.

	μ/m	α	$\frac{\mathcal{R}_\infty}{\hbar\omega}$	σ	R_1	R_2	r_{1s}^∞
TlCl [a]	0.21	4.3	5.2	0.83	1.6	1.5	1.4
CuCl [b]	0.35	3.0	12.5	0.12	1.6	0.6	0.7
ZnO [c]	0.19	1.8	2.2	0.47	1.9	1.3	2.3
CdS [c]	0.14	1.7	1.9	0.26	2.4	1.2	2.9
CuBr [b]	0.20	1.3	7.1	0.20	2.0	0.9	1.3
CdTe [d]	0.08	1.1	1.0	0.29	3.1	1.7	5.1
CuI [e]	0.21	0.77	4.0	0.24	2.0	1.0	1.6
GaAs [d]	0.06	0.28	0.2	0.17	3.9	1.6	15

[a] Reference 19.
[b] Reference 13.
[c] Reference 2.
[d] Reference 20.
[e] Reference 21.

Here the N_i's are the normalization constants and A_i, B_i, and C_i are determined from the orthogonalization condition. Only one additional parameter for each state (α_i, β_i, or γ_i) is determined by the variation of $E_n = \langle \psi_n | H_{\text{ex}} | \psi_n \rangle$. The optimal wave functions and the corresponding energies are then used to calculate the oscillator strengths and absorption coefficients from Eqs. (3.9)–(3.12) or (3.15)–(3.19). More complex wave functions will increase the length of the numerical calculation, but we believe that the main physical effects are already described by the ansatz (4.1).

Before discussing the results for various materials, we will give a general interpretation of the physical effects for typical mass parameters $\mu = 0.2$ m and $\sigma = 0.5(0.1)$. The corresponding polaron radii are $R_1 = 1.83(2.13)\cdot R_{\text{free}}$ and $R_2 = 1.29(0.67)\cdot R_{\text{free}}$, where the free electron polaron radius $R_{\text{free}} = (\hbar/2m\omega)^{1/2}$.

A. Energies of zero-phonon line

In Figs. 1–5 the following quantities are plotted as a function of α for the Coulomb binding parameter $\mathcal{R}_\infty/\hbar\omega = 5$: The exciton energy E_n; the energy difference between s and p states $\Delta E_n = E_{ns} - E_{np}$ $(n = 2, 3)$; the effective Rydberg energy for the nth exciton state $\mathcal{R}_n = \underline{n}^2[(\alpha_1 + \alpha_2)\hbar\omega - E_n]$, where $\alpha_i = \alpha(m_i/m)^{1/2}$ and $\underline{n}$ is the principal quantum number of n; the effective $1s$-state radius $\langle r_{\text{eff}}^{1s} \rangle_n = \langle r \rangle_n/\underline{n}^2$ for s states with $\langle r \rangle_n = \langle \psi_n | r | \psi_n \rangle$; the average virtual phonon number $N_{\text{ph},n} = \langle \Psi_{n,0} | \sum_{\vec{k}} a_{\vec{k}}^\dagger a_{\vec{k}} | \Psi_{n,0} \rangle$.

From these figures it can easily be seen that polaron effects for the $1s$ state are quite different

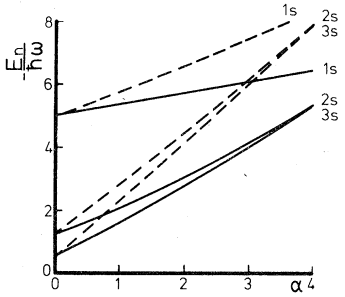

FIG. 1. Exciton energy E_n vs electron-phonon coupling strength α; $\mu/m = 0.2$, $\Re_\infty/\hbar\omega = 5$, and $\sigma = 0.5$ (solid lines) and 0.1 (broken lines).

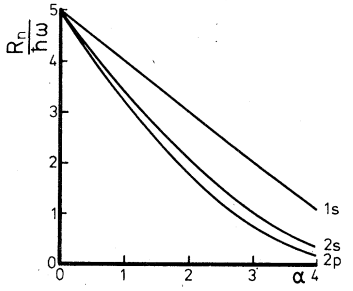

FIG. 3. Effective Rydberg energy $\Re_n$ vs α; $\Re_n = \underline{n}^2[(\alpha_1+\alpha_2)\hbar\omega - E_n]$, where $\underline{n}$ is the principal quantum number of the exciton state n and $\alpha_i = \alpha(m_i/m)^{1/2}$; $\mu/m = 0.2$, $\Re_\infty/\hbar\omega = 5$, and $\sigma = 0.5$.

from those for the excited states. The quantities E_{1s}, $\langle r^{1s}_{\text{eff}}\rangle_{1s}$, and $N_{\text{ph},1s}$ do not change much as a function of α and $N_{\text{ph},1s}$ is smaller by one order of magnitude than $N_{\text{ph},2s}$ and $N_{\text{ph},3s}$. This is explained by the fact that the radius of the 1s state without polaron effects $r_{1s}[=1.5(m\hbar\omega/\mu\Re_\infty)^{1/2}R_{\text{free}}]$ is $1.5\cdot R_{\text{free}}$ for $\mu = 0.2$ m and $\Re_\infty/\hbar\omega = 5$. This is about half the sum of the electron and hole polaron radii $R_1 + R_2 = 3.1$ (or 2.8)$\cdot R_{\text{free}}$. Because of this small radius of the 1s state, the polarization fields of both particles are expected to compensate each other, even if the electron-phonon coupling constant α becomes large. On the other hand, the exciton radius for excited states r_n^∞ $(=r_{1s}^\infty \underline{n}^2$ for s states) is larger than $R_1 + R_2$ and therefore the excited states feel stronger polaron effects with increasing α. We find this situation in many semiconductors (see Table I). This observation is consistent with the small number of the virtual phonons in the 1s state in several polar semiconductors, as shown in PB. We remark here that for $\alpha \geq 4$ and close to the limiting value $\alpha = 5$ ($\mu = 0.2$ m and $\Re_\infty/\hbar\omega = 5$) even the 1$s$ state will show stronger polaron effects.

In Fig. 2 it is seen that s states have lower energy than corresponding p states though the difference is not large. The s-p splitting increases for small α and decreases for larger α. The increase for small α is natural, because s and p states are degenerate for $\alpha = 0$. For larger α the exciton states become more diffuse and their radii become much larger than R_1 and R_2 (see Fig. 4). In this situation the s-p splitting becomes smaller, because the splitting may be considered to originate from the difference of the amplitudes of the s and p wave function in the region $r \leq R_1$ or R_2.

B. Oscillator strength of zero-phonon line

For the allowed transitions in SPA the oscillator strengths are calculated as a function of α. In Fig. 6 the ratio of oscillator strengths $f_n^{(0)}/f_{1s}^{(0)} = |\psi_n(0)|^2 \exp(-g_n)/|\psi_{1s}(0)|^2 \exp(-g_{1s})$ is plotted for the parameter $\Re_\infty/\hbar\omega = 5$. For large α this ratio becomes quite small and deviates considerably from the hydrogenic value (that for $\alpha = 0$). One reason for this deviation is that for increasing α, the excited-state wave functions are much more diffuse than the 1s wave function (Fig. 4). Another reason is the large difference of g_n between the 1s state and excited states, which is shown in Fig. 7. The relative importance of these two ef-

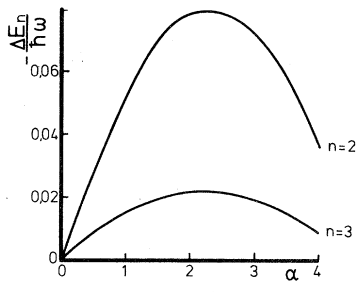

FIG. 2. Energy difference $\Delta E_n = E_{ns} - E_{np}$ $(n = 2, 3)$ vs α; $\mu/m = 0.2$, $\Re_\infty/\hbar\omega = 5$, and $\sigma = 0.5$.

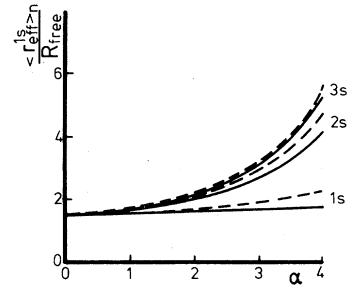

FIG. 4. Effective 1s exciton radius $\langle r^{1s}_{\text{eff}}\rangle_n = \langle r\rangle_n/\underline{n}^2$ (in units of free electron polaron radius R_{free}) vs α; $\langle r\rangle_n$ is the average radius of the exciton state n; $\mu/m = 0.2$, $\Re_\infty/\hbar\omega = 5$, and $\sigma = 0.5$ (solid) and 0.1 (broken).

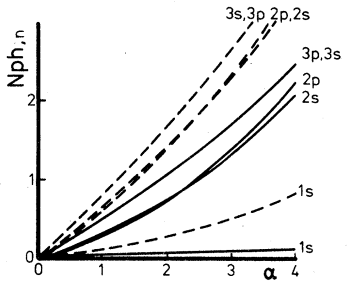

FIG. 5. Average virtual-phonon number $N_{\mathrm{ph},n} = \langle \Psi_{n,0} | \sum_{\vec{k}} a_{\vec{k}}^{\dagger} a_{\vec{k}} | \Psi_{n,0} \rangle$ vs α; $\mu/m = 0.2$, $\Re_\infty/\hbar\omega = 5$, and $\sigma = 0.5$ (solid) and 0.1 (broken).

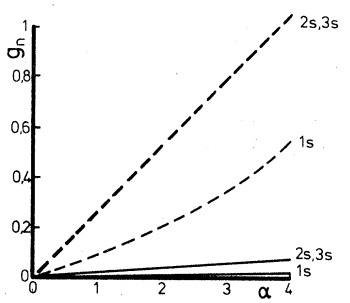

FIG. 7. Factor $g_n = \sum_{\vec{k}} |v_{\vec{k}}|^2 (f_{\vec{k}}^{i} - f_{\vec{k}}^{2})^2$ vs α; $\mu/m = 0.2$, $\Re_\infty/\hbar\omega = 5$, and $\sigma = 0.5$ (solid) and 0.1 (broken).

fects may be estimated from the value of g_n. For $\sigma = 0.5$, g_n is small and the diffuseness of excited states is more important. For a small electron-hole mass ratio $\sigma = 0.1$, g_n is large and quite different for the 1s and the excited states. In this case both effects are important to understand the behavior of the oscillator strength. In Fig. 8 the ratio of the oscillator strengths $f_n^{(0)}/f_{1s}^{(0)}$ is shown as a function of σ for $\alpha = 1$ and 3 and $\Re_\infty/\hbar\omega = 5$. For comparison the ratio of the amplitudes $|\psi_n(0)|^2/|\psi_{1s}(0)|^2$ is also plotted. For small σ it is quite different from the results of the full calculation. This again clearly shows that for the small mass ratios $\sigma \leq 0.4$ the oscillator strength is reduced drastically by the factor $\exp(-g_n)$. We therefore expect an increase in the strength of the phonon side bands.

To complete the picture we have plotted in Fig. 9 the oscillator strength as a function of $\Re_\infty/\hbar\omega$ for $\alpha = 3$ and two different σ. The deviation from the hydrogenic value is largest for the higher states due to the large radii in the higher states.

The different results for $\sigma = 0.5$ and 0.1 in Fig. 9 show again that for $\sigma = 0.1$ the factor $\exp(-g_n)$ is important throughout the region of $\Re_\infty/\hbar\omega$. The actual value of g_n is shown in Fig. 10 for the parameter $\alpha = 3$ and $\sigma = 0.1$. Especially interesting is the state dependency of g_n. For state-independent $f_{\vec{k}}^{i}$, the value for g_n would be a constant for every state and independent of $\Re_\infty/\hbar\omega$. Considering the important role of g_n for the oscillator strength in the case of small electron-hole mass ratios, it is of great importance to have state dependent $f_{\vec{k}}^{i}$ capable of describing the physical situation in much more detail.

Next the forbidden transitions in SPA (or the allowed transitions in TPA) are discussed. For the parameters $\Re_\infty/\hbar\omega = 5$ and $\sigma = 0.5$ (0.1) the oscillator strength ratio $f_{3p,p}^{(0)}/f_{2p,p}^{(0)}$ does not differ too much from the hydrogenic value 0.35 in the region of $0 \leq \alpha \leq 4$ (20% at most). This is in contrast to the large deviation of the oscillator strength ratio $f_{ns}^{(0)}/f_{1s}^{(1)}$ for the allowed transition in SPA. It is explained by the fact that for the parameters chosen, the $2p$ and $3p$ states both have quite spread out wave functions. The polaron effects are nearly the same for these states. This is also seen in the values for g_n (Fig. 11), which are nearly identical for both states. We have also looked at the variation of $f_{3p,p}^{(0)}/f_{2p,p}^{(0)}$ as a function of $\Re_\infty/\hbar\omega$ for $\alpha = 1, 3$ and $\sigma = 0.5$, 0.1. Again the net polaron effects were quite small. The ratio of the oscillator strength $f_{3p,p}^{(0)}/f_{2p,p}^{(0)}$ is

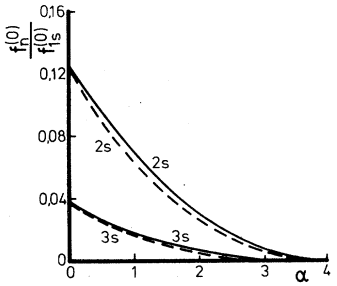

FIG. 6. Ratio of the oscillator strengths of the zero-phonon lines $f_n^{(0)}/f_{1s}^{(0)}$ vs α; $\mu/m = 0.2$, $\Re_\infty/\hbar\omega = 5$, and $\sigma = 0.5$ (solid) and 0.1 (broken).

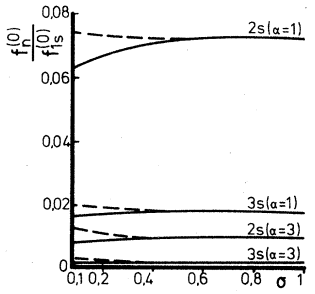

FIG. 8. Ratio of the oscillator strengths of the zero-phonon lines $f_n^{(0)}/f_{1s}^{(0)}$ (as in Fig. 6) vs σ, compared with the ratio of the exciton wave function $|\psi_n(0)|^2/|\psi_{1s}(0)|^2$ (broken); $\mu/m = 0.2$ and $\Re_\infty/\hbar\omega = 5$.

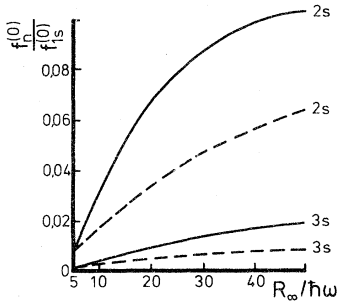

FIG. 9. Ratio of the oscillator strengths of the zero-phonon lines $f_n^{(0)}/f_{1s}^{(0)}$ vs $R_\infty/\hbar\omega$; $\mu/m=0.2$, $\alpha=3$, and $\sigma=0.5$ (solid) and 0.1 (broken).

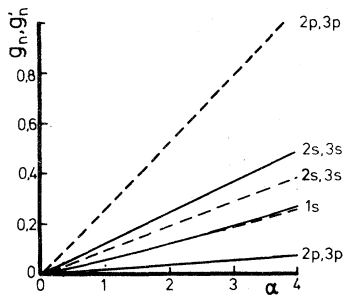

FIG. 11. Factors g_n (for $2p$ and $3p$) and g_n' $=\sum_{\vec{k}}|v_{\vec{k}}|^2 k^2 (s_2 f_{\vec{k}}^1 + s_1 f_{\vec{k}}^2)^2$ (for $1s$, $2s$, and $3s$) vs α; $\mu/m=0.2$, $R_\infty/\hbar\omega=5$, and $\sigma=0.5$ (solid) and 0.1 (broken).

roughly equal to the hydrogenic value within a factor of 2 at most. Therefore we may conclude that the value of the oscillator strength ratio $f_{3p,p}^{(0)}/f_{2p,p}^{(0)}$ is within the difference of some factor from the hydrogenic value and does not change the order of magnitude.

C. Phonon side bands

For the allowed transitions in SPA, only the phonon side band of s states can be observed. The strengths of phonon side bands are governed by g_n as seen from (3.9). Especially this factor is directly given by the ratio of the oscillator strength of the zero-phonon line and its one-phonon side band $g_n=f_n^{(1)}/f_n^{(0)}$. Values of g_n as a function of α have been given in Fig. 7. For large α the oscillator strength of the phonon side band is quite large especially for excited states. It may be noticed that around $\alpha=4$ g_n for $2s$ and $3s$ is about one. This means that the one-phonon side band is as large as the zero-phonon line. The line shape of phonon side bands in the absorption spectra is shown in Fig. 12. The peak positions are drawn in Fig. 13. The following general features can be seen in these figures. A compact wave function produces a broad structure, extended over more than the one-phonon energy in some cases, while a diffuse wave function produces a distinct peak at energies 1.1 to 1.2 $\hbar\omega$ above the zero-phonon line.[22] Therefore, the $1s$-phonon side band has a broad structure, while excited-state phonon side bands produce more pronounced peaks. As an example for $R_\infty/\hbar\omega=20$ the $1s$-phonon side band is very much broader and the height of its peak is lower than that of the much sharper peak of the $2s$-phonon side band, even though the value of the oscillator strength of the one-phonon side band $f_{1s}^{(1)}$ is four times larger than $f_{2s}^{(1)}$. There may be physical situations where the phonon side band of an excited state is easier to observe than that of the $1s$ state.

Finally we discuss the phonon side bands for the forbidden transition in SPA (or for the allowed transition in TPA). In this case it is possible to observe phonon side bands of p- and s-exciton states. The phonon side bands of p states are again governed by the quantity g_n. The value of g_n as a function of α for $R_\infty/\hbar\omega=5$ and $\sigma=0.5$ and 0.1 has been shown in Fig. 11. The value of g_n is quite large for $\sigma=0.1$ and nearly the same for both $2p$ and $3p$ states. Therefore, the phonon side bands of p states are large and in some cases,

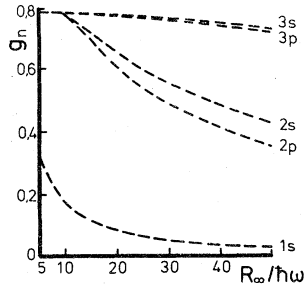

FIG. 10. Factor g_n vs $R_\infty/\hbar\omega$; $\mu/m=0.2$, $\alpha=3$, and $\sigma=0.1$.

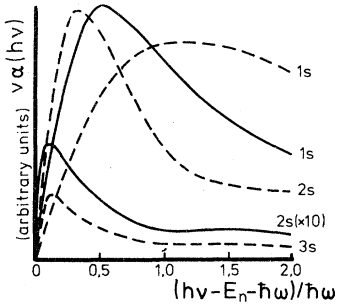

FIG. 12. Line shape $\nu\alpha(h\nu)$ of the phonon side bands in the absorption spectra for allowed transitions in SPA at photon energies $h\nu$; $\mu/m=0.2$, $\alpha=3$, $\sigma=0.1$, and $R_\infty/\hbar\omega=5$ (solid) and 20 (broken).

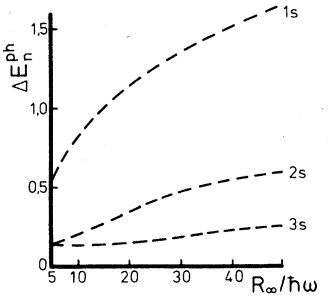

FIG. 13. Peak position of the one-phonon side band, measured from one-phonon energy above the zero-phonon line, $\Delta E_n^{ph} = E_n^{ph} - E_n - \hbar\omega$ vs $R_\infty/\hbar\omega$ for allowed transitions in SPA; ΔE_n^{ph}'s are in units of the phonon energy $\hbar\omega = 1$; $\mu/m = 0.2$, $\alpha = 3$, and $\sigma = 0.1$.

may be as large as the zero-phonon line (for small mass ratios). The general nature of the line shape of the one-phonon side band p states is similar to that for the allowed transition in SPA; for the more diffuse wave function, the more distinct peak appears. Also we see in Fig. 14 that for the change of $R_\infty/\hbar\omega$, the peak position of the line shape for $2p$ and $3p$ states changes in a similar way as for $2s$ and $3s$ for the allowed transition in SPA (in Fig. 13).

The phonon side bands of s excitons are governed by g_n and g_n'. The values of g_n' as a function of α for $R_\infty/\hbar\omega = 5$ and $\sigma = 0.5$, 0.1 have also been shown in Fig. 11. Unlike g_n, the quantity g_n' does not depend much on σ as expected from the expression (3.20), and thus the strength of one-phonon side bands of s excitons does not depend much on σ. The actual strength of the one-phonon side band of $1s$ excitons is expected to be quite large compared to the $2p$ zero-phonon line, as shown in Fig. 15. This reflects the large value of $|\psi_n(0)|^2$ compared to that of $|\partial\psi_{2p}(\vec{r})/\partial\vec{r}|^2_{\vec{r}=0}$. The different nature of the phonon side band for s excitons is also seen in Fig. 14; its peak position changes

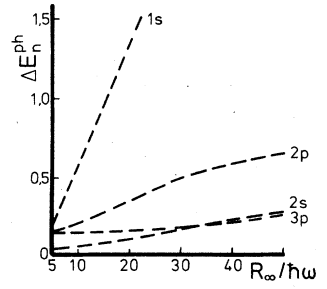

FIG. 14. Peak position of the one-phonon side band, measured from one-phonon energy above the zero-phonon line, $\Delta E_n^{ph} = E_n^{ph} - E_n - \hbar\omega$ vs $R_\infty/\hbar\omega$ for forbidden transitions in SPA (or for allowed transitions in TPA); E_n^{ph}'s are in units of the phonon energy $\hbar\omega = 1$; $\mu/m = 0.2$, $\alpha = 3$, and $\sigma = 0.1$.

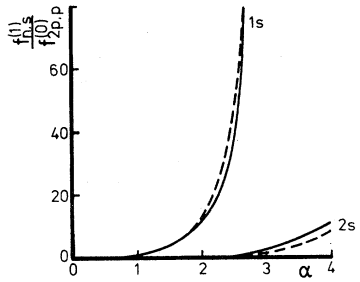

FIG. 15. Ratio of the oscillator strengths of one-phonon side bands of s states and the $2p$ zero-phonon line, $f_{n,s}^{(1)}/f_{2p,p}^{(0)}$ vs α for forbidden transitions in SPA (or for allowed transitions in TPA); $\mu/m = 0.2$, $R_\infty/\hbar\omega = 5$, and $\sigma = 0.5$ (solid) and 0.1 (broken).

differently from that for p states. This reflects different forms of the absorption coefficient for phonon side bands of p and s states, i.e., $\alpha_{n,p}^{(1)}$ and $\alpha_{n,s}^{(1)}$.

V. CUPROUS HALIDES AND CUPROUS OXIDE

In the present section the results of Secs. II and III are applied to cuprous halides CuCl, CuBr, and CuI, and cuprous oxide Cu_2O. It should be noticed that the physical parameters of the cuprous halides are rather different, although these materials have a relatively strong Coulomb binding in common. Because of this wide range of physical parameters and detailed experimental informations on oscillator strengths and phonon side bands in SPA and TPA, cuprous halides provide a good test for the theory. In a previous publication,[13] calculations for CuCl and CuBr in SPA were reported. In the present work, results are presented for SPA and TPA in CuCl, CuBr, and CuI.

The calculations have been performed in the same way as in the previous work,[13] which is described also in Sec. IV but with a finite exchange potential. The following material parameters were used: $\epsilon_0 = 7.43$, 5.7, and 7.6; $\epsilon_\infty = 3.73$, 4.41, and 6.25; $\hbar\omega = 27.2$, 19.8, and 18.6 (meV); $m_1 = 0.392$, 0.24, and 0.262 (m); and $m_2 = 3.17$, 1.2, 1.10 (m) for CuCl, CuBr, and CuI, respectively. It should be noted that values of the masses have been adjusted, so that the theoretical calculation reproduces the experimental energy difference between the $1s$ and $2s$ states, keeping the experimental electron-hole mass ratio σ[23] and the available values of the exchange contribution[24-26] fixed. This procedure has been taken because previous masses[7,8,23] have been determined by the use of Haken's potential for the effective potential between the electron and the hole, which has now been known to be unreliable in a quantitative dis-

TABLE II. Experimental and theoretical values of physical quantities for the single-photon absorption in cuprous halides; zero-phonon energy E_n, its oscillator strength $f_n^{(0)}$, the energy of the peak position of the one-phonon side band E_n^{ph}, its oscillator strength $f_n^{(1)}$, average phonon number $N_{\mathrm{ph},n}$, and average radius $\langle r\rangle_n$. All energies are in meV and relative to E_{1s} and all lengths are in Å.

	E_{2s}	E_{3s}	$\frac{f_{2s}^{(0)}}{f_{1s}^{(0)}}$	$\frac{f_{3s}^{(0)}}{f_{1s}^{(0)}}$	E_{1s}^{ph}	E_{2s}^{ph}	E_{3s}^{ph}	$\frac{f_{1s}^{(1)}}{f_{1s}^{(0)}}$	$\frac{f_{2s}^{(1)}}{f_{1s}^{(0)}}$	$\frac{f_{3s}^{(0)}}{f_{1s}^{(0)}}$	N_{1s}	N_{2s}	N_{3s}	$\langle r\rangle_{1s}$	$\langle r\rangle_{2s}$	$\langle r\rangle_{3s}$
			($\times 10^{-2}$)						($\times 10^{-1}$)							
CuCl																
Expt.[a]	161	179	2.4	0.67	...	190	208	...	8.0	...	...	...	...	...	...	...
Theory	161	177	1.4	0.19	54	195	209	1.5	7.9	8.2	0.20	2.0	2.9	10	51	131
CuBr																
Expt.[b]	84	98	3.3	...	(34)	106	...	...	...	...	...	...	...	...	...	...
Theory	84	96	6.9	1.7	38	109	120	0.3	1.4	1.5	0.06	0.6	0.8	19	83	194
CuI																
Expt.[c]	46	55	(18)	1.8	...	65	...	...	...	...	...	...	...	...	...	...
Theory	46	53	7.5	2.0	33	69	77	0.2	0.7	0.7	0.05	0.4	0.5	24	107	247

[a] Reference 7. [b] Reference 8. [c] Reference 29.

cussion. Mass values obtained in the present work may be considered to be more reliable bare masses. Before presenting our results we remark on the validity of the average denominator approximation for TPA in Sec. III. In the experimental situation for CuCl and CuBr in Refs. 27 and 28, values of k_α in (3.24) are less than about 0.4. Then results of Chap. III may provide a reasonable description for TPA in the present case. In Tables II and III experimental and theoretical values of physical quantities in SPA and TPA are given. The overall agreement is found to be quite good.

The energies of zero-phonon lines of both s and p excitons in SPA and TPA are well reproduced in all materials. The ratio of the oscillator strength of the zero-phonon line differs from experimental values by a factor of 2 or 3. However, we may consider this as a good agreement, since the oscillator strength is a very sensitive test to the actual wave function. To our knowledge there has been no comparable agreement between experiment and theory using the same wave function for energies and oscillator strength. The energies and oscillator strengths of one-phonon side bands are also in good agreement with the available experimental results. Experimentally there have been no assignments for 1s-phonon side bands. As stated in our previous work,[13] we consider that the 1s-one-phonon side band is hidden in the strong spin-orbit split band in CuCl and the previous unidentified peak of 34 meV above E_{1s} is considered as the 1s-one-phonon side band in CuBr. In CuI the present calculations show that the 1s-one-phonon side band is quite weak and has a broad structure whose peak is about 33 meV

TABLE III. Experimental and theoretical values of physical quantities for the two-phonon absorption in cuprous halides; zero-phonon line energy E_n, its oscillator strength $f_{n,p}^{(0)}$, the peak position of the sum of the one-phonon side band of ns and np excitons $E_{n,s+p}^{(1)}$, its oscillator strength $f_{n,s+p}^{(1)}$, average phonon number $N_{\mathrm{ph},n}$, and average radius $\langle r\rangle_n$. All energies are in meV and relative to E_{1s} and all lengths are in Å.

	E_{2p}	E_{3p}	$\frac{f_{3p,p}^{(0)}}{f_{2p,p}^{(0)}}$	$E_{2,s+p}^{\mathrm{ph}}$	$E_{3,s+p}^{\mathrm{ph}}$	$\frac{f_{2,s+p}^{(1)}}{f_{2p,p}^{(0)}}$	$\frac{f_{3,s+p}^{(1)}}{f_{3p,p}^{(0)}}$	N_{2p}	N_{3p}	$\langle r\rangle_{2p}$	$\langle r\rangle_{3p}$
Cucl											
Expt.[a]	168	181	0.38	195	...	...	...	...	...	...	...
Theory	166	179	0.17	199	209	1.3	1.2	2.0	2.9	50	140
CuBr											
Expt.[b]	87	...	...	109	...	...	...	...	...	...	...
Theory	85	97	0.27	110	118	0.32	0.32	0.5	0.8	72	187
CuI											
Theory	46	53	0.31	69	74	0.26	0.23	0.3	0.5	93	237

[a] Reference 27. [b] Reference 28.

above 1s-state E_{1s}. Therefore the 1s-one-phonon side band is considered to contribute to a low-energy tail of 2s exciton. This may explain why the 2s-exciton spectra has an asymmetric shape.[29,30]

The 2s-phonon side bands of SPA in all cuprous halides have been identified experimentally. This may be related to the fact that the 2s-phonon side band generally has a more pronounced peak than the 1s-phonon side band (Sec. IV). Again calculated energies and oscillator strengths for 2s-phonon side bands are in reasonably good agreement with the experiments (Table II). The slightly higher energies of the calculated result might be explained by an interference effect between the phonon side bands and the continuum states which may arise from the part of the Hamiltonian H' neglected in the present calculation. As discussed by Toyozawa,[14] for a strong interference, an exciton-phonon quasibound state (EPQBS) might result and produce the peak at the energy of less than one phonon energy above E_{1s}. However, in cuprous halide the interference effect does not seem to be strong.

It should be noted that in CuCl our calculation has reproduced a 2s-phonon side band as strong as the 2s-zero-phonon line in agreement with the experiment. In Table II this ratio of the zero-phonon line and the phonon side band for the 2s state should be compared with the small ratio for the 1s state. It clearly shows the importance of the state dependence of the f_k^i. If we had used instead a state-independent $f_k^i=(1+R_i^2k^2)^{-1}$, the same value for this ratio would have resulted for any state $f_{ns}^{(1)}/f_{ns}^{(0)}\sim 0.83$ in CuCl. This would mean that the phonon side bands of both the 1s and the 2s states should be as strong as their zero-phonon lines. This is an apparent contradiction to the experiment for the 1s state. The importance of the state dependency can also be understood from the ratio of the exciton radius to the polaron radii R_1 and R_2 as explained in Sec. IV. Values of R_1+R_2 are 26, 41, and 42 Å for CuCl, CuBr, and CuI, respectively. The radius of the 1s state is about half as large as R_1+R_2 and therefore the phonon clouds of the electron and hole largely compensate each other. The radii of the 2s and 3s states are about twice and five times larger than R_1+R_2 and the polaron effects for these excited states are much more effective. This picture is confirmed by the virtual phonon number N_n in the different states (Table II). The values of N_{1s} are one order of magnitude smaller than those for N_{2s} and N_{3s}.

The calculated oscillator strength of the 2s-phonon side band becomes larger with decreasing anionic mass (CuI, CuBr, and CuCl). This is in accordance with the experimental spectra, though explicit numerical values for the oscillator strengths in CuBr and CuI have not been given in experimental works. This tendency is mainly due to the decreasing mass ratio.

The phonon side bands in the TPA are possible for p and s states (Sec. III). Because of the small energy differences of ns and np ($n\geq 2$) exciton states their phonon side bands may overlap. In cuprous halides the calculated oscillator strengths for both p and s states have the same order of magnitude: $f_{2p,p}^{(1)}/f_{2s,s}^{(1)}=1.52$, 0.77, and 0.35 for CuCl, CuBr, and CuI, respectively. The energy of the phonon side band is therefore denoted by $E_{n,s+p}^{\mathrm{ph}}$ (peak position) and its oscillator strength is the sum of the contribution of both states $f_{n,s+p}^{(1)}$. Experimentally these peaks have been assigned as one-phonon side bands of the p state.

The calculated energies $E_{n,s+p}^{\mathrm{ph}}$ do agree quite well with the experimental results. The calculated oscillator strength of the one-phonon side band of both 2s and 2p states is as strong as zero-phonon line of 2p in CuCl and much smaller in CuBr, again in agreement with experiments. In addition the two-phonon side band of 2p and 2s excitons has been observed in CuCl. From our calculation one finds $f_{2,s+p}^{(2)}/f_{2p,p}^{(0)}\sim 0.7$ in accordance with the experiment, although the theoretical line shape is rather broad and not as sharp as in the experiment.

In the present average denominator approximation a large 1s-phonon side band is predicted in TPA: $f_{1s,s}^{(1)}/f_{2p,p}^{(0)}=16$, 1.3, and 1.5 for CuCl, CuBr, and CuI, respectively. Although the theoretical line shape is rather broad with a maximum at about 50 meV above E_{1s} in CuCl we think it should be observable by its large oscillator strength.

Finally, forbidden transitions are discussed in the SPA. A typical material is Cu_2O. It is well known that cuprous oxide shows a very nice hydrogenic series for p states, called the yellow series.[31,32] There are two LO phonons in cuprous oxide both of which have been taken into account in our calculation. All physical parameters used in the calculation have been taken from Ref. 33. The theoretical binding energies of the 2p and 3p states are 23.7 and 10.5 (meV), compared to the experimental values[34] 24.2 and 11.0 (meV). The calculated ratio of the oscillator strength of these zero phonon lines $f_{3p,p}^{(0)}/f_{2p,p}^{(0)}$ is 0.33 and differs very little from the hydrogenic value 0.35 in accordance with the experiment.[31] Values of g_n for the 2p and the 3p states are quite small, only about 2×10^{-3} for both states. Thus the phonon side band of the 2p and 3p states may not be observable. The above results indicate that a detailed consideration of polaron effects is unnecessary for p states. However, for the 1s state

the situation seems to be rather different. The oscillator strength of the one-phonon side band of the 1s state with the high-energy LO phonon (82 meV) turns out to be as large as the 2p zero-phonon line ($f^{(1)}_{1s,s}/f^{(0)}_{2p,p} \sim 0.3$), while that of the low-energy phonon (19 meV) is much smaller ($f^{(1)}_{1s,s}/f^{(0)}_{2p,p} \sim 0.03$).[35] Experimentally the phonon side band of the 1s exciton, called the indirect transition to the 1s exciton, has been considered to make a background absorption for p series.[32,36] Therefore, our result of a large 1s-phonon side band and a very small unobservable phonon side band for p states seems to be consistent with the experiment.

VI. SUMMARY

We have discussed the variational calculation of some optical properties of polar semiconductors such as the transition energies, their oscillator strength, and the absorption coefficient of the exciton zero-phonon line and its phonon side bands. The following general properties of excitons in SPA (TPA) have been found: (1) The Coulomb interaction in the excited exciton states is much more screened than in the ground state (the virtual phonon numbers differ by nearly an order of magnitude). (2) The ratio of the oscillator strength $f^{(0)}_{ns}/f^{(0)}_{1s}$ for the zero-phonon lines in the s states is strongly reduced compared to the hydrogenic value. (3) The corresponding ratio for the forbidden transitions $f^{(0)}_{3p,p}/f^{(0)}_{2p,p}$ is nearly equal to the hydrogenic value. (4) For not too small electron-phonon coupling and small electron-hole mass ratios the phonon side bands of s states and p states in allowed and forbidden (allowed in TPA) transitions, respectively, are quite strong. In some cases the one-phonon side bands for excited states may be as strong as their zero-phonon lines. (5) Phonon side bands of forbidden (allowed in TPA) transitions to s states do not depend very much on the mass ratio and may become quite pronounced.

The detailed calculation for the cuprous halides and cuprous oxide shows good agreement with experimental data. The corresponding wave functions not only yield satisfactory energies, but at the same time reliable oscillator strengths and phonon side bands.

However, one should note that for the excited states there might be some improvements necessary in the strong coupling limit, since the self-energy for large α is not reproduced by our method. For some materials the detailed band structure may be important, like anisotropy[37] and degeneracy.[38] But the general features of the phonon influence as discussed above should not be altered too much by these additional physical effects.

ACKNOWLEDGMENTS

The authors wish to thank F. Mokross and G. Behnke for helpful discussions. One of the authors (M.M.) wishes to thank Professor Suzuoka for making his leave of absence from Yamaguchi University possible. We thank Professor J. D. Dow for his kind interest in this work. The work was partially supported by the Office of Naval Research (Grant No. ONR-N-00014-77-C-0537).

---

*Permanent address: Department of Applied Science, Faculty of Engineering, Yamaguchi University, Ube, Japan 755.

†Present address: Department of Physics and Materials Research Lab, University of Illinois, Urbana, Ill. 61801.

[1]H. Haken, *Polarons and Excitons*, edited by C. G. Kuper and D. G. Whitfield (Oliver and Boyd, Edinburgh, 1963), p. 302 and references therein.

[2]J. Pollmann and H. Büttner, Solid State Commun. 17, 1171 (1975); Phys. Rev. B 16, 4480 (1977).

[3]S. D. Mahanti and C. M. Varma, Phys. Rev. B 6, 2209 (1972).

[4]E. O. Kane, Phys. Rev. B 18, 6849 (1978).

[5]M. Matsuura and C. Mavroyannis, J. Low Temp. Phys. 28, 129 (1977).

[6]S. Bednarek, J. Adamowski, and M. Suffczynski, Solid State Commun. 21, 1 (1977).

[7]J. Ringeissen, A. Coret, and S. Nikitine, in *Localized Excitations in Solids* (Plenum, New York, 1968), p. 297.

[8]S. Lewonczuk, J. Ringeissen, and S. Nikitine, J. Phys. (Paris) 32, 941 (1971).

[9]Y. Toyozawa, J. Lum. 1,2, 732 (1970).

[10]G. Ascarelli, in *Polarons in Ionic Crystals and Polar Semiconductors*, edited by J. T. Devreese (North-Holland, Amsterdam, 1972), p. 161.

[11]J. Dillinger, Č. Koňák, V. Prosser, J. Sak, and M. Zvára, Phys. Status Solidi B 29, 707 (1968); J. Sak, Phys. Rev. Lett. 25, 1654 (1970).

[12]H. Sumi, J. Phys. Soc. Jap. 36, 770 (1974); 38, 825 (1975).

[13]M. Matsuura and H. Büttner, Solid State Commun. (to be published).

[14]Y. Toyozawa and J. Hermanson, Phys. Rev. Lett. 21, 1637 (1968); J. Hermanson, Phys. Rev. B 2, 5043 (1970); Y. Toyozawa, in Proceedings of the Third International Conference on Photoconductivity, Stanford, California, 1969, p. 151 (unpublished).

[15]J. O. Dimmock, in *Semiconductors and Semimetals*, edited by P. K. Willardson and A. C. Beer (Academic, New York, 1967), Vol. 3, p. 259.

[16]G. D. Mahan, Phys. Rev. 170, 825 (1968).
[17]R. Loudon, *The Quantum Theory of Light* (Clarendon, Oxford, 1973), p. 304.
[18]K. C. Rustagi, F. Pradere, and A. Mysyrowicz, Phys. Rev. B 8, 2721 (1973).
[19]Calculated from the recent values of $\mu^* = 0.347$. [J. Nakahara, Solid State Commun. 29, 115 (1979) in a similar way as in Ref. 5.]
[20]S. Wang and M. Matsuura, Phys. Rev. B 10, 3330 (1974).
[21]Determined in Sec. V of the present work.
[22]The pronounced peak is more characteristic for the state independent f_k^i [$= (1+R_i^2k^2)^{-1}$].
[23]C. I. Yu, T. Goto, and M. Ueta, J. Phys. Soc. Jap. 34, 693 (1973); Y. Kato, T. Goto, T. Fujii, and M. Ueta, *ibid*. 36, 169 (1974).
[24]The exchange contribution for 1s state ΔE_{1s}^{ex} is taken to be 8 meV for CuCl, $\frac{8}{3} \sim 3$ meV for CuBr from Refs. 25 and 26. For CuI ΔE_{1s}^{ex} is taken to be zero because of no available information. This may not be considered to be serious, as seen in results of Theories I and II in Table I of Ref. 13.
[25]Y. Kato, C. I. Yu, and T. Goto, J. Phys. Soc. Jap. 28, 104 (1970).
[26]W. Staude, Phys. Status Solidi B 43, 367 (1971).
[27]A. Bivas, C. Marange, J. B. Grun, and C. Schwab, Opt. Commun. 6, 142 (1972).
[28]C. Marange, A. Bivas, R. Levy, J. B. Grun, and C. Schwab, Opt. Commun. 6, 138 (1972).
[29]C. Jung, S. Lewonczuk, J. Ringeissen, and S. Nikitine, Rev. Phys. Appl. 7, 43 (1972).
[30]The overlap of the 1s-one-phonon side band and 2s-zero-phonon line in CuI may also contribute to the large experimental value of the oscillator strength ratio $f_{2s}^{(0)}/f_{1s}^{(0)}$ (in Table III) compared to the theoretical value.
[31]S. Nikitine, in *Optical Properties of Solids*, edited by S. Nudelman and S. S. Mitra (Plenum, New York, 1969), p. 197.
[32]V. T. Agekyan, Phys. Status Solidi A 43, 11 (1977).
[33]M. Matsuura, J. Phys. C 10, 3345 (1977).
[34]M. A. Washington, A. Z. Genack, H. Z. Cummins, R. H. Bruce, A. Compaan, and R. A. Forman, Phys. Rev. B 15, 2145 (1977).
[35]These numbers should be considered to be rough values because the present crystal parameters with the exchange constant $J = 0$ yield the smaller 1s-binding energy 103 (meV) compared to the experimental value 139 (meV).
[36]In experiments, not only LO phonons with the energy of 82 meV but also other types of phonons (e.g., phonons with 13 meV) contribute to the rather large background absorption in SPA.
[37]H. Fock, B. Kramer, and H. Büttner, Phys. Status Solidi B 72, 155 (1975).
[38]H. R. Trebin, Phys. Status Solidi B 92, 601 (1979).